750893

A Comparison of Results Obtained With Different Analytical Techniques for Reconstruction of Highway Accidents

Raymond R. McHenry
Transportation Safety Dept., Calspan Corp.

THE ANALYTICAL TECHNIQUES that have traditionally been applied in reconstructions of highway accidents have predominently been "closed-form" calculations based on piecewise linear solutions of the equations of motion. The refinement of such approximation techniques has been hampered by the limited available response data from staged collisions and spinout trajectories. In the presently reported research, a refined closed-form calculation procedure has been developed through the use, in part, of time-history data generated with the Simulation Model of Automobile Collisions (SMAC) computer program (1-7).*

The SMAC program employs a step-by-step integration technique with which time-

This paper is based on research performed under Contract Nos. DOT-HS-053-3-609 and DOT-HS-053-3-658 with the National Highway Traffic Safety Administration, U.S. Department of Transportation and Contract No. MVMA, CAL 7505-C4.11 with the Motor Vehicle Manufacturers Association. The contents of the paper reflect the views of the author, who is responsible for the facts and accuracy of the data presented herein, and do not necessarily reflect the official views or policy of the Department of Transportation or the Motor Vehicle Manufacturers Association.

*Numbers in parenthesis designate References at end of paper.

ABSTRACT

For several staged collisions, results obtained with closed form reconstruction calculations and with a computerized step-by-step procedure are compared with measured responses. A refined, closed-form reconstruction procedure is defined, derivations of the analytical relationships are outlined and detailed results of sample applications are presented.

Closed form calculation procedures for estimating impact conditions became a topic of interest in relation to the development of an automatic starting routine for iterative applications of the Simulation Model of Automobile Collisions (SMAC) computer program. The accuracy of initial estimates of speeds determines the total number of iterative adjustments of SMAC that are required to achieve an acceptable overall match of the evidence. Since a high degree of success was achieved in the refinement of such calculation procedures, the end product, by itself, is considered to be a valuable aid to accident investigations.

histories of vehicle responses in collisions and spinout trajectories are generated. In applications of that program, successive estimates of initial conditions are tested by means of comparisons of predicted and measured physical evidence.

In the Calspan mobile accident investigation system (7) a simplified, closed-form calculation routine (START) was programmed to automatically generate initial approximations of the collision conditions to start iterative runs of the SMAC computer program. The START routine includes a major subroutine, SPIN1, which is based on relationships defined by Marquard (8) for approximating the energy dissipated during spinout trajectories involving combined linear and angular velocities. In addition, it includes application of the principle of conservation of linear momentum (subroutine OBLIQUE) and, for the case of axial collisions where the spinout trajectories do not permit approximation of impact conditions on the basis of conservation of momentum alone, it includes a simplified analysis of vehicle damage (subroutine AXIAL).

The presently reported development is a separate computer program (i.e., as opposed to a "starting" routine) based on START, which is aimed at applications to cases in which the reported evidence is not sufficiently detailed to justify application of the SMAC program and/or to existing large bodies of case reports where the cost per case for analytical reconstruction is a primary consideration. This development, the Calspan Reconstruction of Accident Speeds on the Highway (CRASH) computer program, includes significant improvements in the accuracy of the START approximations.

The Marquard relationships for spinout trajectories (8) were extended on the basis of a detailed analysis of the results of a number of SMAC runs. Incorporation of a capability to handle a residual linear velocity at the end of the yawing rotation was found to substantially improve accuracy. Also, the use of empirical coefficients which are functions of the initial ratio of linear to angular velocity was found to yield significant improvements.

The interpretation of damage data in CRASH is an extension of the single-vehicle frontal collision approach of Campbell (9) to include two vehicles and general collision conditions. It makes use of the Vehicle Damage Index (VDI) as defined in (10) and it includes provisions for use of supplementary damage details when they are available.

The CRASH program is designed to accommodate a range of accident evidence, from VDIs only at one extreme to complete definitions of rest and impact positions as well as damage dimensions at the other. Multiple outputs of speed change and/or impact speed are provided with identification of the basis for each approximation. In this manner, it is possible for the user to select the approximation result based on the most reliable items of evidence while assuring that the various different items of evidence are at least grossly compatible.

The overall objective of the reported development is the same as that of the SMAC program. It is aimed at achieving uniformity in the interpretation of physical evidence from automobile accidents. In particular, the speed-change, ΔV, and its direction are believed to be the best indicators of exposure severity for the vehicle occupants. While the SMAC program has been demonstrated to yield reconstructed impact speed accuracies in the range of $\pm$ 5% its full benefits are achieved only with complete and accurate definitions of the scene evidence and it costs approximately $20 per run. The on-scene use of SMAC is strongly recommended in new investigations as a means of insuring completeness, compatibility and accuracy of the scene measurements. In relation to the overall costs of an investigation, the use of SMAC would involve a relatively small increase. In fact, the scene sketch and the reconstruction calculations and sketch produced by the on-scene SMAC system may more than offset the costs of corresponding off-scene efforts in reporting investigated cases.

In existing case reports, the frequently fragmentary reporting of scene data may not justify the costs of SMAC applications. Also, the large number of available case reports makes the cost per case for additional processing an important consideration. Therefore, the CRASH program, which has been demonstrated to yield $\pm$ 12% accuracy of speed estimates in reasonably well-documented cases at a computer cost of only approximately $5.00 per case, is believed to fill an existing need for a low cost accident reconstruction aid.

In the following, results obtained with the CRASH program are compared with experimental data and SMAC results for a number of collision configurations. The detailed analytical relationships that are used in the CRASH program are then presented and discussed.

COMPARISON OF RESULTS

Results of staged collisions that are suitable for use in evaluation of reconstruction techniques are relatively scarce. Many of the staged collisions for which at

least partial response data are available include unrealistic effects from the viewpoint of reconstruction. For example, the extensively documented series of intersection-type collisions reported by Severy, et al, in (13) involve the following unrealistic effects and/or data gaps.

(1) In many of the tests, full braking was applied abruptly, late in the spinout trajectories. However, the corresponding tire mark data are not reported and details of the brake applications in individual tests are not defined.

(2) The vehicles were towed toward the collision point with the transmissions in neutral. As a result, there was no engine braking during the spinouts.

(3) The tire-pavement friction coefficient was not measured.

(4) Damage dimensions are not reported.

(5) Speed-change data are not reported.

In car-to-car collisions staged by Calspan as a part of research in structural crashworthiness, the rest positions were not measured and the striking vehicle was "snubbed" subsequent to the impact by a trailing cable at a deceleration level substantially larger than that of full braking. Also, the struck vehicle was motionless at impact, making the collision conditions not representative of typical highway accidents.

As a result of the above difficulties with available measured response data, it has been necessary to use a "shotgun" approach in evaluating the validity of the developed techniques. Comparisons have been made with a large number of staged collisions, each of which has some shortcomings as a "standard", well-defined and representative accident. From a scientific viewpoint, this approach leaves much to be desired. It does not permit levels of confidence to be established in a rigorous manner. Rather, it merely indicates approximate error ranges in general applications. The results of four sample applications are presented and discussed in the following paragraphs.

In some of the presented comparisons, the measured data have been supplemented with SMAC-generated damage or rest position data. Footnotes on the comparison tables define the use of such supplementary "evidence".

In relation to the comparisons, differences that exist in the analytical treatments of crush properties in the SMAC and CRASH programs should be noted. The SMAC program includes a coefficient of restitution based on data presented in (12) whereas the CRASH program uses a non-zero impact velocity intercept at zero residual crush to approximate the same effect. When actual damage dimensions are available, the error ranges of the two separate approximation techniques can be directly compared. However, in one of the presented comparisons for which damage information is not available, SMAC-generated damage data have been used as the basis for the CRASH approximation.

Offset Frontal (Table 1) - This experimental collision produced relatively large magnitudes of crush, and it is considered to be a good test of the damage analysis procedure within the CRASH program for an offset collision. However, the presence of sand around the impact point creates uncertainty regarding the effective tire-ground friction coefficient. The sand was applied to the surface in an attempt to reduce tire-terrain friction and to more clearly delineate tire mark evidence, since the vehicles were not braked and skid marks were expected to be minimal.

The SMAC program was applied as a "forward" calculation, starting with the known speeds at impact. In Table 1 it may be seen that the SMAC and CRASH values for the speed changes, ΔV, of the two vehicles are in very close agreement. The value for ΔV that is listed under the SPIN II (Appendix 1) heading of CRASH is based primarily on the DAMAGE-generated value, as a result of the axial nature of the collision. The actual speed changes of the vehicles were not measured.

The CRASH reconstructions of the speeds at impact are considered to be reasonably close to the measured values, particularly in view of the uncertainty regarding the effective value of the tire-terrain friction coefficient.

90° Rear-Side Impact at 40 MPH (Table 2) - The iteration of SMAC for this case made use of the position and orientation of Vehicle #2 at 1.0 second subsequent to the collision contact, rather than at its reported rest position outside the quadrant painted on the test area pavement ((13), Figure 7D). This approach was selected in view of the well-defined spin-out trajectories within the painted quadrant and the undefined nature of the late brake application. The trajectory portion of CRASH necessarily made use of the reported rest position of Vehicle #2. It should be noted, however, that the rest orientation of Vehicle #2 is not defined in (13) and had to be estimated. Because of the absence of VDIs and damage dimensions, SMAC-generated data were used for the damage analysis portion of CRASH. The tire-ground friction coefficient was estimated on the basis of SMAC and CRASH results for several of the individual tests in the series.

Table 1

COLLISION CONFIGURATION Offset Frontal

TEST IDENTIFICATION Calspan MRA #1

	MEASURED			SMAC			CRASH		
							SPIN II		DAMAGE
	SPEED AT IMPACT	ΔV	VDI	SPEED AT IMPACT	ΔV	VDI	SPEED AT IMPACT	ΔV	ΔV
	MPH	MPH		MPH	MPH		MPH	MPH	MPH
VEHICLE #1	30.5	-	12FYEW4	(30.5)*	34.2	12FYEW5	34.1 (+11.8%)	32.8	32.5
VEHICLE #2	31.5	-	12FYEW5	(31.5)*	26.7	12FYEW5	34.4 (+ 9.2%)	25.4	25.3

	REST POSITIONS			IMPACT POSITIONS			END OF ROTATIONAL AND/OR LAT. SKIDDING				ROLLING RESISTANCE				TIRE-PAVEMENT
	X'_{CR}	Y'_{CR}	ψ_R	X'_{CS}	Y'_{CS}	ψ_S	X'_{CI}	Y'_{CI}	ψ_I						
	FT.	FT.	DEG.	FT.	FT.	DEG.	FT.	FT.	DEG.	ROT.	RF	LF	RR	LR	μ
VEHICLE #1	-7.3	4.2	-25.0	-8.4	1.0	0.0	-	-	-	CCW	0.0	1.0	0.0	0.0	(0.5)
VEHICLE #2	0.7	-2.5	162.5	8.4	-1.0	180.0	-	-	-	CCW	0.0	1.0	0.0	0.0	SAND

MEASURED DAMAGE DIMENSIONS

	WIDTH	DAMAGE EXTENT				MOMENT ARM		DIRECTION			
	LI	CI1	CI2	CI3	CI4	DI	RATIO	ANGI	VEH. SIZE	VEH. WGT. LBS	REFERENCE
	IN.	IN.	IN.	IN.	IN.	IN.	RHOI	DEG.			
VEHICLE #1	34.0	46.5	(35.8)	(25.2)	14.5	-22.5	-	360°	3.	3080.	2, 15
VEHICLE #2	35.0	57.0	(49.8)	(42.7)	35.5	-22.0	-	360°	3.	3950.	

*Forward Calculation with Known Speeds.

Table 2

COLLISION CONFIGURATION 90° Rear-Side at 40 MPH

TEST IDENTIFICATION UCLA ITTE Side Impact Series

	MEASURED			SMAC			CRASH		
							SPIN II		DAMAGE
	SPEED AT IMPACT	ΔV	VDI	SPEED AT IMPACT	ΔV	VDI	SPEED AT IMPACT	ΔV	ΔV
	MPH	MPH		MPH	MPH		MPH	MPH	MPH
VEHICLE #1	40.0	-	-	40.3 (+ 0.8%)	11.0	01FDEW3	37.3 (- 6.8%)	14.7	12.9*
VEHICLE #2	40.0	-	-	41.0 (+ 2.5%)	10.6	10LZEW3	39.6 (- 1.0%)	14.7	12.9*

	REST POSITIONS			IMPACT POSITIONS			END OF ROTATIONAL AND/OR LAT. SKIDDING				ROLLING RESISTANCE				TIRE-PAVEMENT
	X'_{CR}	Y'_{CR}	ψ_R	X'_{CS}	Y'_{CS}	ψ_S	X'_{CI}	Y'_{CI}	ψ_I						
	FT.	FT.	DEG.	FT.	FT.	DEG.	FT.	FT.	DEG.	ROT.	RF	LF	RR	LR	μ
VEHICLE #1	50.0	-21.0	-147	-13.3	0.0	0.0	39.0	-20.0	-173	CCW	1.0	0.0	0.0	0.0	(0,8)
VEHICLE #2	19.8	-60.9	(-336)	0.0	-5.25	-90.0	-	-	-	CCW	0.0	0.0	1.0	1.0	

MEASURED DAMAGE DIMENSIONS *

	WIDTH	DAMAGE EXTENT				MOMENT ARM		DIRECTION			
	LI	CI1	CI2	CI3	CI4	DI	RATIO	ANGI	VEH. SIZE	VEH. WGT. LBS	REFERENCE
	IN.	IN.	IN.	IN.	IN.	IN.	RHOI	DEG.			
VEHICLE #1	(76.8)	(12.0)	(14.0)	(14.0)	(24.0)	(0,0)	-	-	3.	-	13, Fig. 7D
VEHICLE #2	(96.7)	(0.0)	(12.7)	(14.3)	(14.2)	(-71,23)	-	-	3.	-	

*SMAC-Generated Damage Dimensions Used in CRASH,

The SMAC and CRASH reconstructions of speeds at impact are considered to be in excellent agreement with the measured values. While the actual speed changes of the vehicles were not measured, the three sets of estimates are in generally good agreement with each other. It is obvious that each reconstruction technique is within range of being "tweaked" into agreement, via minor refinements, when improved experimental data are available.

Frontal, Head-On, Large Vs. Small (Table 3) - The fact that ΔV of each vehicle was measured in this experimental crash makes it of interest for the present comparison purposes. It was a relatively severe event, having a closing speed of approximately 88 miles per hour between a full-size and a compact vehicle.

The primary physical evidence consists of the damage dimensions and the vehicle weights. The striking vehicle was "snubbed" by a trailing cable subsequent to the collision, and the rest position of the struck vehicle was not measured.

An earlier SMAC calculation based on this collision was reported in (2), in which it was concluded that the effective coefficient of restitution generated by the SMAC program was too large. Additional SMAC runs performed within the present research effort have revealed that the accuracy of SMAC implementation of the input specification for structural recovery is significantly affected by time increment size in this particular collision configuration. It was found that the use of a very small collision time increment (0.0005 sec.) tended to increase the effective coefficient of restitution by prolonging the total duration of the collision contact. With collision time increments larger than approximately 0.002 second, the solution stability was found to be adversely affected. Thus, a need is indicated for some further development of the SMAC routine within which partial structural recovery is implemented.

The SMAC results shown in Table 3 were obtained with a collision time increment of 0.0015 second and with the "typical automobile frontal" inputs for coefficient of restitution of (7). The errors for ΔV are not considered to be representative of the general accuracy of predictions by the SMAC simulation. Rather, they reflect the cited difficulty with accurate control of the effective coefficient of restitution in SMAC for this collision configuration.

In the absence of rest position information, SMAC-generated data for rest and impact positions were used for the trajectory analysis portion of CRASH. It should be noted that the smaller vehicle did not rotate in yaw any appreciable amount in the presented SMAC prediction. In the cited earlier run (2) and in runs performed within the present effort where the effective coefficient of restitution was too large, 180° of yaw rotation of that vehicle occurred. While moving backward with its front wheels locked by damage the vehicle is, of course, directionally unstable. Therefore, a relatively small disturbance in its heading direction can readily produce 180° of yaw rotation.

The CRASH reconstruction of the speeds at impact, based on the SMAC-predicted rest positions, benefits from the fact that the SMAC and DAMAGE predictions of speed changes are in close agreement with each other.

In view of the large extents of damage to the two vehicles and the fact that vehicles of different sizes were involved, the correlation of reconstruction results with experimental data and the agreement among the different analytical techniques are considered to be very good.

Oblique Side Impact (Table 4) - The occurrence of two separate impacts makes this experimental crash of particular interest. The SMAC and CRASH reconstructions of the speeds at impact for this case are considered to be in very good agreement with the measured values.

While the actual speed changes were not measured, the three sets of estimates are in good agreement with each other. The CRASH value for the speed change of Vehicle #1 reflects the underestimate of the impact speed of Vehicle #2. Since damage dimensions were not recorded, the damage analysis portion of CRASH made use only of vehicle weights, sizes and investigator-rated VDIs. Therefore, it is considered to be the least reliable of the sets of speed-change estimates. The reported values of ΔV are the vector sums of the results of two separate applications of CRASH for the two sets of VDIs.

DAMAGE ANALYSIS

Hand calculation techniques for damage analysis that yield reasonable estimates of the impact velocity in frontal collisions (i.e., the relative velocity of approach) have been developed by Emori (full width contact only, (11)) and by Campbell (partial width contact, (9)), using linear approximations of the relationship between residual crush and impact velocity. The SMAC program (1-7) applies a similar analytical approach to the entire peripheral structure, and it has been demonstrated to yield good approximations of both impact velocity and speed change, ΔV, in general collision configurations including oblique,

non-central impacts. The objective of the present research has been to develop a simple, closed-form damage analysis technique that is applicable to general collision configurations.

Table 3

COLLISION CONFIGURATION Frontal, Head-On, Large vs, Small

TEST IDENTIFICATION Calspan Test No. 14

	MEASURED			SMAC			CRASH		
							SPIN II		DAMAGE
	SPEED AT IMPACT	ΔV	VDI	SPEED AT IMPACT	ΔV	VDI	SPEED AT IMPACT	ΔV	ΔV
	MPH	MPH		MPH	MPH		MPH	MPH	MPH
VEHICLE #1	43.8	63.8	12FDEW6	(43.8)*	68.1 (+6.7%)	12FDEW5	44.1** (+ 0.7%)	67.0 (+ 5.0%)	67.0 (+ 5.0%)
VEHICLE #2	43.8	26.3	12FDEW2	(43.8)*	30.6 (+16.3%)	12FDEW3	44.5** (+ 1.6%)	29.6 (+12.5%)	29.6 (+12.5%)

	REST POSITIONS**			IMPACT POSITIONS*			END OF ROTATIONAL AND/OR LAT. SKIDDING			ROLLING RESISTANCE				TIRE-PAVEMENT
	X'_{CR}	Y'_{CR}	ψ_R	X'_{CS}	Y'_{CS}	ψ_S	X'_{CI}	Y'_{CI}	ψ_I					μ
	FT.	FT.	DEG.	FT.	FT.	DEG.	FT.	FT.	DEG.	ROT.	RF	LF	RR	LR	
VEHICLE #1	(-51,9)	(0.0)	(-1.2)	(-8.0)	(0,0)	(0.0)	-	-	-	(CCW)	1.0	1.0	0.0	0.0	(0.8)
VEHICLE #2	(-12.6)	(0,0)	(180.6)	(5.9)	(0,0)	(180.0)	-	-	-	(CCW)	1.0	1.0	0.0	0.0	

MEASURED DAMAGE DIMENSIONS

	WIDTH	DAMAGE EXTENT				MOMENT ARM		DIRECTION		VEH. SIZE	VEH. WGT. LBS	REFERENCE
	LI	C11	C12	C13	C14	DI	RATIO	ANGI				
	IN.	IN.	IN.	IN.	IN.	IN.	RHOI	DEG.				
VEHICLE #1	62.2	41.	41.	41.	41.	0.0	1.0	360°		1.	1750.	14, 2
VEHICLE #2	62.2	23.	23.	23.	23.	0.0	1.0	360°		4.	3960.	

*Forward Calculation with Known Speeds,

**SMAC-Generated Rest and Impact Dimensions.

Table 4

COLLISION CONFIGURATION Oblique Side Impact

TEST IDENTIFICATION Calspan MRA #3

	MEASURED			SMAC			CRASH		
							SPIN II		DAMAGE
	SPEED AT IMPACT	ΔV	VDI	SPEED AT IMPACT	ΔV	VDI	SPEED AT IMPACT	ΔV	ΔV
	MPH	MPH		MPH	MPH		MPH	MPH	MPH
VEHICLE #1	33.0	-	01RFEE2 02RZEW3	32.7 (- 1.0%)	16.3*	02RFEW3 03RZEW2	32.3 (- 2.1%)	13.4	12.9*
VEHICLE #2	32.5	-	08LFEW3 08LZEW2	31.8 (-2.2%)	12.5*	10LYEW3 09LZEW3	28.9 (-11.1%)	12.4	12.4*

	REST POSITIONS			IMPACT POSITIONS			END OF ROTATIONAL AND/OR LAT. SKIDDING				ROLLING RESISTANCE				TIRE-PAVEMENT
	X'_{CR}	Y'_{CR}	ψ_R	X'_{CS}	Y'_{CS}	ψ_S	X'_{CI}	Y'_{CI}	ψ_I						
	FT.	FT.	DEG.	FT.	FT.	DEG.	FT.	FT.	DEG.	ROT.	RF	LF	RR	LR	μ
VEHICLE #1	33.0	-17.0	-51.0	-0.5	-2.0	0.0	-	-	-	CCW	1.0	1.0	1.0	1.0	0.77
VEHICLE #2	43.0	- 8.0	-39.0	6.5	7.5	-48.	-	-	-	CCW	1.0	1.0	1.0	1.0	

	MEASURED DAMAGE DIMENSIONS										
	WIDTH	DAMAGE EXTENT				MOMENT ARM		DIRECTION			
	LI	CI1	CI2	CI3	CI4	DI	RATIO	ANGI	VEH. SIZE	VEH. WGT. LBS	REFERENCE
	IN.	IN.	IN.	IN.	IN.	IN.	RHOI	DEG.			
VEHICLE #1	-	-	-	-	-	-	-	-	3.	3095.	2
VEHICLE #2	-	-	-	-	-	-	-	-	3.	3338.	

*Vector Sum of ΔV From Two Separate Impacts.

Central Collisions - In the case of central collisions (i.e., where the line-of-action of the collision force passes through the centers of masses of the two vehicles, Figure 1) the extents and areas of residual crush on the two vehicles provide a basis for estimating the relative velocity at impact of the vehicles. The following simplified linear analysis provides relationships for such estimates.

In Figure 1, the symbols are defined as follows.

M_1, M_2 = Masses of Vehicles 1 and 2, lb sec^2/in,

K_1, K_2 = Linear approximations of peripheral crush stiffness of contact areas of Vehicles 1 and 2, for increasing load, lb/in

X_1, X_2 = Displacements of centers of masses, inches.

X = Displacement of peripheral interface, inches.

In the following derivation, the time derivative of a variable is indicated by a dot over the symbol for the variable, and the subscript zero is used to indicate the initial value of a variable at zero time.

Application of Newton's Second Law to the system depicted in Figure 1 yields

$$M_1\ddot{X}_1 = -\left(\frac{K_1K_2}{K_1+K_2}\right)(X_1-X_2) \qquad (1)$$

$$M_2\ddot{X}_2 = \left(\frac{K_1K_2}{K_1+K_2}\right)(X_1-X_2) \qquad (2)$$

To facilitate solution of equations (1) and (2), let $\delta = X_1-X_2$, $\dot{\delta}_0 = \dot{X}_{10}-\dot{X}_{20}$. Then equations (1) and (2) can be restated as

$$\ddot{\delta} + \left(\frac{K_1K_2}{K_1+K_2}\right)\left(\frac{M_1+M_2}{M_1M_2}\right)\delta = 0 \qquad (3)$$

Solving (3) for the maximum relative displacement,

$$(\delta)_{max} = (\dot{X}_{10}-\dot{X}_{20})\sqrt{\frac{(K_1+K_2)\,M_1M_2}{K_1K_2\,(M_1+M_2)}} \text{ inches} \qquad (4)$$

Let $\delta_1 = X_1-X$, $\delta_2 = X-X_2$. For force equilibrium,

$$K_1\delta_1 = K_2\delta_2 \text{ lbs} \qquad (5)$$

and, by definition,

$$\delta_1+\delta_2 = \delta \text{ inches} \qquad (6)$$

Solution of (5) and (6) for δ_1 yields

$$\delta_1 = \left(\frac{K_2}{K_1+K_2}\right)\delta \text{ inches} \qquad (7)$$

Equation (4) can be restated in the following form,

$$\dot{X}_{10}-\dot{X}_{20} = \sqrt{\frac{(M_1+M_2)\,K_1K_2(\delta)^2_{max}}{M_1M_2\,(K_1+K_2)}} \text{ in/sec} \qquad (8)$$

From (7), (6) and (5),

$$\dot{X}_{10}-\dot{X}_{20} = \sqrt{\frac{(M_1+M_2)(K_1\delta_1^2+K_2\delta_2^2)}{M_1M_2}} \text{ in/sec} \qquad (9)$$

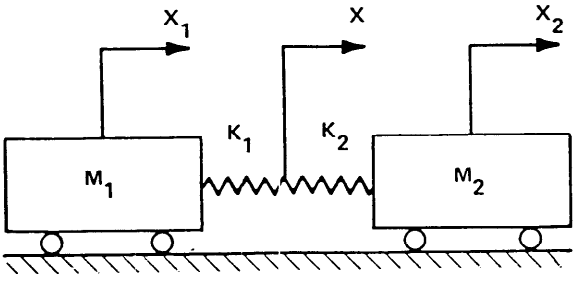

Fig. 1-Schematic reconstruction of central collision

The energy absorbed in peripheral crush of Vehicles 1 and 2 can be expressed as

$$E_1 = \frac{1}{2}K_1\delta_1^2 \text{ lb in} \qquad (10)$$

$$E_2 = \frac{1}{2}K_2\delta_2^2 \text{ lb in} \qquad (11)$$

Substitution of (10) and (11) into (9) yields

$$\dot{X}_{10}-\dot{X}_{20} = \sqrt{\frac{(M_1+M_2)\,2\,(E_1+E_2)}{M_1M_2}} \text{ in/sec} \qquad (12)$$

From Conservation of Momentum, the common velocity, V_c, may be obtained.

$$V_c = \frac{M_1\dot{X}_{10}+M_2\dot{X}_{20}}{M_1+M_2} \text{ in/sec} \qquad (13)$$

The velocity changes experienced by Vehicles 1 and 2 during the approach period of the collision are

$$\Delta V_1 = \dot{X}_{10}-V_c = \left(\frac{M_2}{M_1+M_2}\right)(\dot{X}_{10}-\dot{X}_{20}) \text{ in/sec} \qquad (14)$$

$$\Delta V_2 = V_c - \dot{X}_{20} = \left(\frac{M_1}{M_1+M_2}\right)(\dot{X}_{10} - \dot{X}_{20}) \text{ in/sec} \quad (15)$$

From (14), (15) and (12), these velocity changes (approach period) can be expressed as

$$\Delta V_1 = \sqrt{\frac{2(E_1+E_2)}{M_1\,(1+M_1/M_2)}} \text{ in/sec} \quad (16)$$

$$\Delta V_2 = \sqrt{\frac{2(E_1+E_2)}{M_2\,(1+M_2/M_1)}} \text{ in/sec} \quad (17)$$

Non-Central Collisions - In the more general case of non-central collisions, a common velocity is achieved at the regions of collision contact rather than at the centers of gravity. For example, in the offset frontal collision depicted in Figure 2, a common velocity is reached at point P.

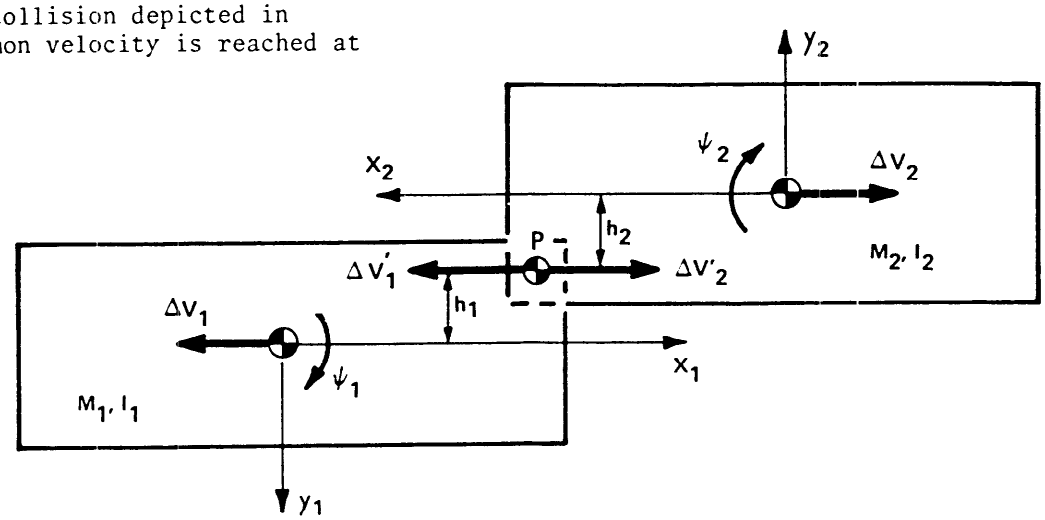

Fig. 2-Offset frontal collision

In Figure 2, the collision force acting on Vehicle 1,

$$F_x = -M_1\ddot{X}_1 = -M_1(\ddot{X}_p - h_1\ddot{\psi}_1) \quad (18)$$

The corresponding moment acting on Vehicle 1,

$$F_x h_1 = -I_1\ddot{\psi}_1 = -M_1 k_1^2\ddot{\psi}_1 \quad (19)$$

where k_1^2 = radius of gyration squared of Vehicle 1 in yaw, in^2.

From (19), the angular acceleration of Vehicle 1,

$$\ddot{\psi}_1 = -\frac{F_x h_1}{M_1 k_1^2} \quad (20)$$

Substitution of (20) in (18) yields

$$\ddot{X}_p = -\frac{F_x}{M_1}\left(\frac{k_1^2+h_1^2}{k_1^2}\right) \quad (21)$$

$$\ddot{X}_1 = -\frac{F_x}{M_1} = \left(\frac{k_1^2}{k_1^2+h_1^2}\right)\ddot{X}_p \quad (22)$$

Let $\gamma_1 = \dfrac{k_1^2}{k_1^2+h_1^2}$, then from (22),

$$\ddot{X}_1 = \gamma_1\ddot{X}_p \quad (23)$$

Integration of equation (23) over the time interval during which a common velocity is reached at point P yields

$$\Delta\dot{X}_1 = \gamma_1\Delta\dot{X}_p, \text{ or} \quad (24)$$

$$\Delta V_1 = \gamma_1\Delta V_1' \quad (25)$$

where $\Delta V_1'$ is the velocity change during the approach period of the collision at point P.

From (21), the effective mass of Vehicle 1 acting at point P may be expressed as $\gamma_1 M_1$. Similarly, the effective mass of Vehicle 2 acting at point P may be expressed as $\gamma_2 M_2$. Substitution of the effective masses into equations (16) and (17) yields expressions for the velocity changes (approach period) at point P.

$$\Delta V_1' = \sqrt{\frac{2(E_1+E_2)}{\gamma_1 M_1\,(1+\gamma_1 M_1/\gamma_2 M_2)}} \text{ in/sec} \quad (26)$$

$$\Delta V_2' = \sqrt{\frac{2(E_1+E_2)}{\gamma_2 M_2(1+\gamma_2 M_2/\gamma_1 M_1)}} \quad \text{in/sec} \qquad (27)$$

From equation (25) and the corresponding expression for Vehicle 2, the velocity changes (approach period) at the center of gravity of the two vehicles are obtained.

$$\Delta V_1 = \sqrt{\frac{2\gamma_1(E_1+E_2)}{M_1(1+\gamma_1 M_1/\gamma_2 M_2)}} \qquad (28)$$

$$\Delta V_2 = \sqrt{\frac{2\gamma_2(E_1+E_2)}{M_2(1+\gamma_2 M_2/\gamma_1 M_1)}} \qquad (29)$$

It should be noted that when $\gamma_1 = \gamma_2 = 1.00$, equations (28) and (29) reduce to the central-impact relationships of equations (16) and (17).

In Figure 3, further relationships required to approximate the effects of intervehicle friction are depicted.

In Figure 3, the effect of intervehicle friction on the direction of the resultant collision force is depicted. The dimensions h_1 and h_2 are approximated on the basis of (1) the midpoint of the collision contact region, (2) the existence of a tangential velocity (columns 1 and 2 of the VDI), and (3) the intervehicle friction coefficient, μV.

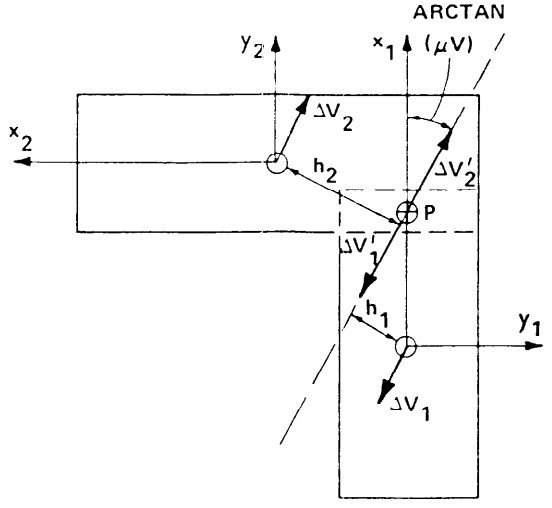

Fig. 3-Intersection collision

In the cited study by Emori (11) and in the SMAC program (2) a simple friction coefficient has been shown to yield reasonable approximations of collision responses. Inherent in the present analytical treatment is the assumption that the residual crush provides a direct measure of the energy absorbed by compressive forces between the two vehicles and that the additional work done by tangential shear forces does not provide directly measurable damage evidence. It should be noted that the front end of the impacting vehicle in an intersection collision is generally distorted laterally, but that corresponding measurement techniques have not been established.

Absorbed Energy - The calculation of absorbed energy is based on residual crush and is patterned after that developed by Campbell (9). The only significant difference is in the treatment herein of the energy absorbed without residual crush as being proportional to the contact width rather than a constant. The following relationship is applied,

$$E_i = \int_0^{W_0} \left(A_i C + \frac{B_i C^2}{2} + G_i\right) dw \quad \text{in lbs} \qquad (30)$$

where E_i = Energy absorbed by vehicle i, inch lbs.

$C = f(w)$ = Residual crush of vehicle i, inches.

w = Width dimension of damaged region, inches.

A_i, B_i, G_i = Empirical coefficients of unit width properties obtained from crash test data.

Values for A_i, B_i and G_i, corresponding to the energy absorbed in barrier crashes with "standard" test weights, are stored in a table that is categorized for four vehicle sizes and for the front, side and rear of each vehicle size (Table 5). It should be noted that the frontal values in Table 5 are based on Campbell's data but that the side and rear data are gross approximations only, that are based on fragmentary crash test data. Actual vehicle weights are used in the solution of equations (28) and (29).

The developed calculation procedure permits a four-point definition of the damage profile. By default, four-point definitions are generated on the basis of column 7 of the VDI and on three "representative" types of damage profiles. The integration of equation (30) is based on trapezoidal approximations of the damage region, yielding the following equation.

$$E_i = \frac{L_i}{3}\left[\frac{A_i}{2}(C_{i1}+2C_{i2}+2C_{i3}+C_{i4}) + \frac{B_i}{6}(C_{i1}^2+2C_{i2}^2+2C_{i3}^2+C_{i4}^2+C_{i1}C_{i2}+C_{i2}C_{i3}+C_{i3}C_{i4}) + 3G_i\right] \quad \text{inch lbs} \qquad (31)$$

for approximating the initial linear and angular (yaw) velocities of a vehicle in a spinout trajectory (i.e., at the point of separation subsequent to a collision) on the basis of the energy dissipated during its changes in position and orientation between separation and rest. He includes the cases of freely rotating wheels and of locked wheels, each with the front wheels limited to the straight ahead position of steering.

Table 5

DAMAGE DATA

Coeff. For Equation (30)		SUB COMPACT	COMPACT	INTER-MEDIATE	FULL SIZE	UNITS
		1.	2.	3.	4.	
COL. 3 = F	A	130.5	154.6	281.8	307.5	LB/INCH
	B	58.72	69.57	33.82	36.89	LB/INCH^2
	G	144.94	171.78	1174.3	1281.1	LB
COL. 3 = R, L	A	82.21	111.8	43.72	49.19	LB/INCH
	B	42.76	58.16	47.23	53.13	LB/INCH^2
	G	79.04	107.5	20.24	22.77	LB
COL. 3 = B	A	65.98	78.18	85.51	93.28	LB/INCH
	B	13.20	15.64	17.11	18.66	LB/INCH^2
	G	164.97	195.45	213.78	233.21	LB

The "equivalent barrier speed" as defined by Campbell (9) is not equal to the speed change, ΔV, in low speed collisions, since the rebound velocity produced by the coefficient of restitution is not included. At the velocity intercept of the linearized fit of impact velocity plotted against residual crush, elastic behavior is indicated for the vehicle crush. The total speed change, ΔV, should, therefore, be equal to twice the impact velocity in that velocity range, in the absence of an energy absorbing bumper device.

The impact speeds without residual crush that are indicated by Campbell's linear fits (no actual data points at impact speeds below 15 MPH) suggest substantially higher coefficients of restitution than, for example, the values presented by Emori in (12). Without more definitive information on the actual magnitude and variation of the coefficient of restitution as a function of both deflection extent and position on the vehicle periphery, the complexity of introducing a corresponding refinement in the damage analysis technique cannot be justified. Therefore, the damage analysis procedure defined herein tends to underestimate ΔV in low speed collisions.

SPINOUT ANALYSIS

In (8), Marquard defines relationships

In the case of freely rotating wheels, the linear and angular velocities of the vehicle are decelerated alternately as the heading direction changes with respect to the direction of the linear velocity. When the vehicle slides laterally, the side forces at the front and rear tires tend to have the same direction despite the existence of a yaw velocity. Therefore, during this phase of the motion, the angular velocity tends to remain constant while the linear velocity is decelerated. When the longitudinal axis is aligned with the direction of the linear velocity, the side forces at the front and rear tires act in opposite directions and the angular velocity is decelerated while the linear velocity tends to remain constant. A SMAC-generated example of the time-histories of angular and linear velocity, for the case of no braking, is shown in Figure 4. Marquard defines a different form of solution for the case of locked wheels, whereby the ratio of angular to linear displacement during the spinout is used to determine empirical coefficients.

The derivation of equations in (8) is not completely presented. Therefore, some details of the assumptions must be deduced from the final form of the equations.

In the following outline of the derivation, the time derivative of a variable is indicated by a dot over the symbol for the variable and the subscript S is used

to indicate the value of a variable at the point of separation.

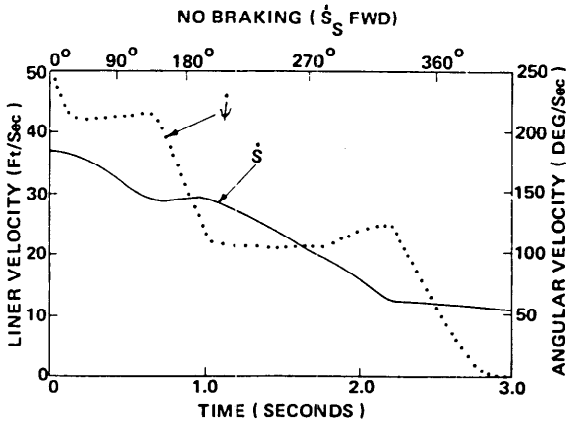

Fig. 4-Linear and angular velocity versus time

Spinout Without Braking - In Figure 5, an idealized plot of the time histories of linear and angular velocities is depicted. The symbols T_1 and T_2 are used to represent the times, subsequent to separation, at which the linear and angular velocities, respectively, reach zero values. The areas under the velocity plots are, of course, equal to the corresponding linear and angular displacements. If it is assumed that reasonable approximations of the areas under the two velocity plots can be obtained from the triangles shown in Figure 5 as broken lines, the following relationships can be applied.

$$\Delta\psi \cong \left(\frac{\dot{\psi}_s}{2}\right) T_1, \text{ and} \qquad (32)$$

$$S \cong \left(\frac{\dot{S}_s}{2}\right) T_2 \qquad (33)$$

During the periods of angular deceleration, the magnitude of that deceleration can be approximated as

$$\ddot{\psi} \cong \frac{\mu g}{k^2}\left(\frac{a+b}{2}\right) \qquad (34)$$

where μ = nominal tire-ground friction coefficient.

g = acceleration of gravity, in/sec^2.

k^2 = radius of gyration squared for complete vehicle in yaw, in^2.

$(a+b)$ = wheelbase, inches.

From equation (34) the actual deceleration time of the angular velocity can be approximated as

$$t_1 = \frac{\dot{\psi}_s}{\ddot{\psi}} = \frac{2\dot{\psi}_s k^2}{\mu g(a+b)} \qquad (35)$$

During the linear deceleration portion of the motion (i.e., for orientations near that of broadside sliding), the tire side forces, which are perpendicular to the wheel planes, act at a changing angle with respect to the direction of the linear velocity. If the average value of the cosine of the angle during that portion of the motion is taken to be 0.85, the average magnitude of the linear deceleration during periods of linear deceleration can be approximated as

$$\ddot{S} \cong 0.85\ \mu g \qquad (36)$$

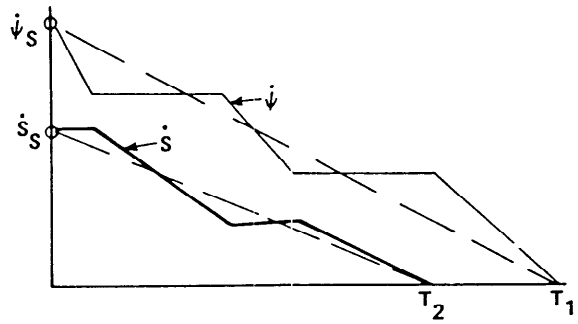

Fig. 5-Idealized plot of velocities versus time

The corresponding actual deceleration time of the linear velocity can be approximated by

$$t_2 = \frac{\dot{S}_s}{\ddot{S}} = \frac{\dot{S}_s}{0.85\ \mu g} \qquad (37)$$

The total time required to stop both the linear and the angular motions can be expressed, from equations (35) and (37) as

$$T = t_1 + t_2 = \frac{2\dot{\psi}_s k^2}{\mu g(a+b)} + \frac{\dot{S}_s}{0.85\ \mu g} \qquad (38)$$

If it is assumed that both phases of the motion end at approximately the same time,

$$T \approx T_1 \approx T_2, \text{ then from (32) and (33),}$$

$$\frac{2(\Delta\psi)}{\dot{\psi}_s} \approx \frac{2S}{\dot{S}_s} \approx T \qquad (39)$$

From (39),

$$\frac{\dot{S}_s}{\dot{\psi}_s} \approx \frac{S}{\Delta\psi} \qquad (40)$$

Substitution of (39) and (40) into (38) yields

$$\frac{2(\Delta\psi)}{\dot{\psi}_s^2} = \frac{2k^2}{(a+b)\,\mu g} + \frac{S}{0.85\,\mu g \Delta\psi} \qquad (41)$$

Solution of (41) for $\dot{\psi}_s$ yields

$$\dot{\psi}_s = \sqrt{\frac{\mu g (\Delta\psi)^2}{\frac{k^2}{(a+b)}\left|\Delta\psi\right| + \frac{S}{1.70}}}\ \operatorname{sgn}(\Delta\psi) \qquad (42)$$

From (38) and (39),

$$\dot{S}_s = 1.70\left[\frac{\mu g(\Delta\psi)}{\dot{\psi}_s} - \frac{k^2\left|\dot{\psi}_s\right|}{(a+b)}\right] \qquad (43)$$

Equations (42) and (43) correspond to the relationships defined by Marquard in (8). The relationships defined by (42) and (43) were extended to include the case of partial braking, in the following manner.

If θ is used to define the decimal portion of full deceleration produced by braking or wheel damage, where $0 \leq \theta \leq 1.00$, a linear deceleration of $0.85\,\theta\mu g$ occurs during t_1, the deceleration time of the angular velocity. Therefore, the linear velocity to be decelerated in the corresponding phase of motion is reduced to

$$\dot{S}_1 = \dot{S}_s - 0.85\,\theta\mu g t_1 \qquad (44)$$

The total time required for linear deceleration is reduced to

$$t_2 = \frac{\dot{S}_1}{0.85\,\mu g} = \frac{\dot{S}_s}{0.85\,\mu g} - \theta t_1 \qquad (45)$$

Therefore, the total time required to stop both the linear and the angular motions becomes

$$T = t_1 + t_2 = \frac{\dot{S}_s}{0.85\mu g} + (1-\theta)\,\frac{2\dot{\psi}_s k^2}{(a+b)\mu g} \qquad (46)$$

With the introduction of θ, equations (42) and (43) become

$$\dot{\psi}_s = \sqrt{\frac{\mu g\,(\Delta\psi)^2}{\left(\frac{k^2}{a+b}\right)\left|\Delta\psi\right|(1-\theta) + \frac{S}{1.70}}}\ \operatorname{sgn}\Delta\psi \qquad (47)$$

$$S_s = 1.70\left[\frac{\mu g\,(\Delta\psi)}{\dot{\psi}_s} - \frac{k^2\left|\dot{\psi}_s\right|(1-\theta)}{(a+b)}\right] \qquad (48)$$

Application of equations (47) and (48) to a number of SMAC-generated spinout trajectories revealed several shortcomings. First, it was found that a residual linear velocity frequently exists at the end of the rotational motion. Thus, equations (39) and (40) can introduce large errors. Next it was found that the shapes of the plots of linear and angular velocity vs. time change substantially as functions of the initial ratio of linear to angular velocity, affecting the accuracy of simple linear approximations of the areas under the curves. Finally, the transitions between the different deceleration rates in the linear and angular motions do not occur abruptly. Rather, slope changes in the plots of velocities against time occur gradually, producing rounded "corners" in the curves (e.g., see Figure 4). As a result of the transitions, the effective deceleration rates in the two modes of motion are somewhat smaller than those corresponding to the full value of tire-ground friction.

To improve the accuracy of the approximations, provision was made for introduction of a residual linear velocity at the end of the rotational motion and empirical coefficients, in the form of polynomial functions of the initial ratio of linear to angular velocity. Since that velocity ratio is initially unknown, a solution procedure was developed whereby several trial values of the ratio, based on an approximate equation, are used to obtain multiple solutions. The solution for which the velocity ratio most closely matches the corresponding trial value is retained. The residual linear velocity is approximated on the basis of the distance traveled subsequent to the end of the rotational motion. The corresponding derivation of equations is outlined in the following.

The total time required to stop the angular motion is approximated by

$$T_1 = \alpha_1\,\frac{\Delta\psi}{\dot{\psi}_s} = t_1 + t_2 \qquad (49)$$

The actual time of angular deceleration,

$$t_1 = \frac{2\dot{\psi}_s k^2}{(a+b)\mu g \alpha_2} \qquad (50)$$

The actual time during which linear acceleration occurs,

$$t_2 = \frac{(\dot{S}_s - \dot{S}_1)}{\alpha_4 \mu g} - \frac{\alpha_3 \theta t_1}{\alpha_4} \quad (51)$$

The change in linear velocity during time T_1, can be approximated as

$$S_1 = \left(\frac{\dot{S}_s + \dot{S}_1}{\alpha_5}\right) T_1 \quad (52)$$

From (49) and (52)

$$\alpha_1 \frac{\Delta\psi}{\dot{\psi}_s} = \alpha_5 \frac{S_1}{(\dot{S}_s + \dot{S}_1)} \quad (53)$$

From (49), (50) and (51),

$$\alpha_1 \frac{\Delta\psi}{\dot{\psi}_s} = \frac{2\dot{\psi}_s k^2}{(a+b)\mu g \alpha_2}\left(1 - \frac{\alpha_3\theta}{\alpha_4}\right) + \frac{\dot{S}_s - \dot{S}_1}{\alpha_4 \mu g} \quad (54)$$

From (53),

$$(\dot{S}_s - \dot{S}_1) = \frac{\alpha_5}{\alpha_1} \frac{S_1 \dot{\psi}_s}{\Delta\psi} - 2\dot{S}_1 \quad (55)$$

Substituting (55) in (54),

$$\dot{\psi}_s^2 + B\,\dot{\psi}_s + C = 0 \quad (56)$$

where

$$B = \frac{\dot{S}_1 \left|\Delta\psi\right|}{D} \quad (57)$$

$$C = \frac{\alpha_1 \alpha_4 \mu g (\Delta\psi)^2}{2D} \quad (58)$$

$$D = \frac{\alpha_4 k^2 \left|\Delta\psi\right| \left(1 - \frac{\alpha_3\theta}{\alpha_4}\right)}{\alpha_2 (a+b)} + \frac{\alpha_5 S_1}{2\alpha_1} \quad (59)$$

From (54)

$$\dot{S}_s = \dot{S}_1 + 2\alpha_4 \left\{ \frac{\alpha_1 \mu g \Delta\psi}{2\dot{\psi}_s} - \frac{\dot{\psi}_s k^2 \left(1 - \frac{\alpha_3\theta}{\alpha_4}\right)}{(a+b)\alpha_2} \right\} \quad (60)$$

The detailed solution procedure for equations (56) through (60) is outlined in Appendix 1. It should be noted that the developed equations reduce to the form of (47) and (48) when the residual linear velocity is set to zero and the coefficients, α_i, are set to constant values. Also, the developed relationships apply to the case of fully locked wheels as well as rotating wheels, eliminating the need for a separate "locked wheel" procedure such as that defined in (8).

CONCLUDING REMARKS

The described closed-form calculation procedure of the CRASH program, which was initially developed as a starting routine for the SMAC computer program, has been shown to be capable of yielding impact velocity approximations with a ± 12% accuracy. The operating cost ranges from only $1.00 to $5.00 per case, depending on the extent of the available case data. Thus, the CRASH program, by itself, is considered to be a valuable aid to accident investigation in cases (1) where the evidence is not sufficiently complete to justify the larger costs of the SMAC program or (2) where large numbers of existing accident reports are to be processed to obtain uniformly derived, low-cost estimates of impact velocities and velocity changes. The availability of the SMAC computer program to generate detailed collision response data has been highly beneficial to the described development.

ACKNOWLEDGEMENTS

The author wishes to acknowledge contributions of Mr. James P. Lynch to development of the format and coding of the CRASH computer program. Also, the work of Dr. Ian S. Jones and Mrs. Camille F. Bainbridge on START, the predecessor to CRASH, contributed directly to the success of the present research.

REFERENCES

1. R. R. McHenry, "Development of a Computer Program to Aid the Investigation of Highway Accidents," Calspan Report No. VJ-2979-V-1, December 1971 (PB #208537, Contract No. FH-11-7526).

2. R. R. McHenry, D. J. Segal, J. P. Lynch, and P. M. Henderson, "Mathematical Reconstruction of Highway Accidents," Calspan Report No. ZM-5096-V-1, January 1973 (PB #220150, Contract No. DOT-HS-053-1-146).

3. J. A. Bartz, D. J. Segal, and R. R. McHenry, "Mathematical Reconstruction of Accidents - Analytical and Physical Reconstruction of Ten Selected Highway Accidents," Calspan Report No. ZQ-5341-V-1, March 1974 (Contract No. DOT-HS-053-3-658).

4. R. R. McHenry, "A Computer Program for Reconstruction of Highway Accidents," paper presented at the 17th Stapp Car Crash Conference, November 12-13, 1973.

5. I. S. Jones and D. J. Segal, "The

Application of the SMAC Accident Reconstruction Program to Actual Highway Accidents," paper presented to the American Association for Automotive Medicine, 13 September 1974.

6. I. S. Jones, "Results of Selected Applications to Actual Highway Accidents of the SMAC Reconstruction Program" paper presented at the 18th Stapp Car Crash Conference, December 1974.

7. R. R. McHenry, I. S. Jones and J. P. Lynch, "Mathematical Reconstruction of Highway Accidents - Scene Measurement and Data Processing System," Calspan Report No. ZQ-5341-V-2, December 1974 (Contract No. DOT-HS-053-3-658).

8. E. Marquard, "Progress in the Calculations of Vehicle Collisions," Automobiltechnische Zeitschrift, Jahrq. 68, Heft 3, 1966, pp. 74-80.

9. K. L. Campbell, "Energy Basis for Collision Severity," SAE Paper No. 740565, Proceedings of the 3rd International Conference on Occupant Protection, Troy, Michigan, July 10-12, 1974.

10. "Collision Deformation Classification," Society of Automotive Engineers Technical Report J224a, 1972.

11. R. I. Emori, "Analytical Approach to Automobile Collisions," SAE Paper No. 680016, Automotive Engineering Congress, Detroit, Michigan, January 8-12, 1968.

12. R. I. Emori, "Mechanics of Automobile Collisions," First International Conference on Vehicle Mechanics," Wayne State University, Detroit, Michigan, July 16-18, 1968.

13. D. M. Severy, J. H. Mathewson, and A. W. Siegel, "Automobile Side-Impact Collisions, Series II," SAE SP-232.

14. N. J. DeLeys, D. J. Segal, and J. S. Patten, "Underride/Overide of Automobile Front Structures in Intervehicular Collisions," Volume 2 "Car-to-Car Head-On Impacts," Calspan Report No. VJ-2844-V-3, December 1971.

15. J. A. Bartz and F. E. Butler, "A Three-Dimensional Computer Simulation of a Motor Vehicle Crash Victim - Phase 2 - Validation Study of the Model," Calspan Report No. VJ-2978-V-2, December 1972.

APPENDIX 1

Subroutine SPIN II

Inputs:

X'_{c1}, Y'_{c1}, ψ_1 = Position and orientation at end of rotation (feet and degrees).

X'_{cs}, Y'_{cs}, ψ_s = Position and orientation at separation (feet and degrees).

$\dot{S}_1$ = Residual linear velocity at end of rotation (ft/sec).

a+b = Wheelbase, inches.

k^2 = Radius of gyration squared for complete vehicle in yaw, in^2.

μ = Nominal tire-ground friction coefficient.

θ = Decimal portion of full deceleration, $0 \leq \theta \leq 1.000$.

g = Acceleration of gravity = 386.4 inches/sec^2.

1. $S_1 = 12\sqrt{(X'_{c1}-X'_{cs})^2+(Y'_{c1}-Y'_{c2})^2}$ inches

2. $\Delta\psi = \dfrac{(\psi_1-\psi_s)}{57.3}$ radians

3. $\gamma_s = \arctan\left(\dfrac{Y'_{c1}-Y'_{cs}}{X'_{c1}-X'_{cs}}\right)$

4. For $\theta = 1.0$,

$$\rho' = 1.408\left(\frac{S_1}{|\Delta\psi|} - 32\right)$$

For $\theta < 1.0$,

$$\rho' = \frac{-b + \sqrt{b^2-4ac}}{2a}$$

where $a = (1-\theta)\ 8.52\times10^{-4}$

$b = 0.94-0.23\theta$

$c = 40.64-8.64\theta - \dfrac{S_1}{|\Delta\psi|}$

5. $\rho_1 = 0.70\rho'$
$\rho_2 = 0.85\rho'$
$\rho_3 = \rho'$
$\rho_4 = 1.15\rho'$
$\rho_5 = 1.30\rho'$

6. For each ρ_j, calculate α_{ij}, where

$i = 1,2,3,4,5$
$j = 1,2,3,4,5$

For $0 \leq \rho_j \leq 250$,

$$\alpha_{ij} = a_{i0}+a_{i1}\rho_j+a_{i2}\rho_j^2+a_{i3}\rho_j^3$$

For $250 < \rho_j$,

$$\alpha_{ij} = K_i$$

where

	i				
	1	2	3	4	5
a_0	2.58	0.88	0.2417	0.671	1.223
a_1	-7.44×10^{-3}	-3.92×10^{-3}	4.85×10^{-3}	1.4772×10^{-3}	1.7307×10^{-2}
a_2	1.504×10^{-5}	8.0×10^{-6}	-9.667×10^{-6}	-4.50×10^{-6}	-1.053×10^{-4}
a_3	0	0	0	5.80×10^{-9}	1.993×10^{-7}
K	1.66	0.400	0.850	0.850	2.08

7. $$D_j = \left\{ \frac{\alpha_{4j} k^2 |\Delta\psi| \left(1 - \frac{\alpha_{3j}\theta}{\alpha_{4j}}\right)}{\alpha_{2j}(a+b)} + \frac{\alpha_{5j} S_1}{2\alpha_{ij}} \right\}$$

8. $$B_j = \frac{12\dot{S}_1 |\Delta\psi|}{D_j}$$

9. $$C_j = \frac{\alpha_{1j}\alpha_{4j}\mu g (\Delta\psi)^2}{2D_j}$$

10. $$\dot{\psi}_{sj} = \left\{ \frac{B_j}{2} + \frac{1}{2}\sqrt{B^2{}_j + 4C_j} \right\} \text{sgn } (\Delta\psi) \text{ rad/sec}$$

11. $$\dot{S}_{sj} = 12\dot{S}_1 + 2\alpha_{4j} \left\{ \frac{\alpha_{1j}\mu g(\Delta\psi)}{2\dot{\psi}_{sj}} - \frac{|\dot{\psi}_{sj}| k^2 \left(1 - \frac{\alpha_{3j}\theta}{\alpha_{4j}}\right)}{(a+b)\alpha_{2j}} \right\}$$

inches/sec

12. $$\beta_j = \frac{\rho_j |\dot{\psi}_{sj}|}{\dot{S}_{sj}} - 1$$

Let n = the value of j for which $|\beta_j|$ is smallest.

13. $\dot{\psi}_s = 57.3\ \dot{\psi}_{sn}$ degrees/sec

14. $\dot{S}_s = \dot{S}_{sn}$ inches/sec

15. $U_s = \dot{S}_s \cos(\gamma_s - \psi_s)$ inches/sec

16. $V_s = \dot{S}_s \sin(\gamma_s - \psi_s)$ inches/sec

17. Return with starting values:

U_s inches/sec

V_s inches/sec

$\dot{\psi}_s$ degrees/sec